Journal of Alloys and Compounds, 213/214 (1994) 106–110
JALCOM 4011

Alloying behavior in selected neptunium binary systems: the role of 5f bonding

J.K. Gibson, R.G. Haire and M.M. Gensini
Oak Ridge National Laboratory, P.O. Box 2008, Oak Ridge, TN, 37831-6375 (USA)

T. Ogawa
Japan Atomic Energy Research Institute, Tokai-mura, Ibaraki-ken 319-11 (Japan)

Abstract

We have undertaken to establish the phase relations for selected binary alloy systems of Np with another actinide or with a d-block transition metal. Empirical data obtained by differential thermal analysis and powder X-ray diffraction have been supplemented by elementary modeling procedures and correlations with similar alloy systems to propose the primary features of selected phase diagrams. The initial focus of these investigations has been on the Np–Am, Np–Zr and, most recently, the Np–Fe systems. The findings for the former two systems are summarized, and preliminary results for the Np–Fe system are reported. The potential role of 5f bonding in determining alloying behavior is discussed in conjunction with regular-solution model predictions to address unique features evident in certain Np alloy systems.

1. Introduction

Empirical knowledge of the alloying behavior of transuranium actinides remains inadequate as a result in part of the scarcity and intense radioactivity of these elements [1]. Because of their technological importance and availability, the phase relations in U and Pu binary alloy systems are generally better established than those in the corresponding Np systems. The chemistry of the light actinides (An) (*e.g.* Pa, U, Np and Pu), is complex, reflecting the accessibility of multiple oxidation states and the potential for involvement of 5f electrons in bonding. The metallurgy of these elements is similarly complex [2] and it is imprudent to predict their alloying behavior without some empirical basis for modeling the bonding of an actinide in the specific metallic environment. The nature and degree of alloying between two actinide metals, or between an actinide and a d block transition metal, is also a potential indicator of the influence and/or involvement of the 5f electrons in metallic bonding. There is a renewed interest in phase relations in actinide alloy systems owing to potentials for technologies such as nuclear transmutation of long-lived isotopes and advanced fuel recycling schemes.

We have used differential thermal analysis (DTA) together with room temperature powder X-ray diffraction (XRD) to elucidate important features of the phase diagrams of selected binary alloy systems containing Np. The initial focus of these studies was on the Np–Am and Np–Zr systems, while current efforts involve the Np–Fe system. We present here a summary of the previous experimental results for the Np–Am [3] and Np–Zr [4, 5] systems, together with a suggested form for the Np–Zr phase diagram. Some preliminary results for the Np–Fe system are also presented and discussed in comparison with the U–Fe and Pu–Fe systems. An explanation for the unanticipated phase relations found in the Np–Zr system, in particular, is developed using regular-solution model considerations.

2. Experimental details

The details of the DTA apparatus and procedures were described previously [4]. As with the earlier DTA studies of the Np–Zr [4, 5] and Np–Am [3] alloy systems, the Np–Fe alloy samples were prepared from the component metals by two methods: *in situ* by fusion in the DTA apparatus, or *ex situ* by arc melting. The neptunium metal (^{237}Np) was prepared by calcium reduction of NpF_4 and contained less than 200 wt. ppm cationic impurities, as determined by spark source mass spectrometric analysis. The iron metal was a commercial product (wire) rated at 99.9985% purity. The DTA analyzer (Perkin–Elmer DTA1700) was operated to a maximum temperature of about 1450 °C. Room temperature powder XRD analysis of selected alloy spec-

SSDI 0925-8388(93)04011-E

imens was performed using Debye–Scherrer cameras. Further details of the experimental approach for the Np–Fe studies will be presented later in a subsequent report [6].

3. Results and discussion

The important features of the Np–Zr and Np–Am alloy systems are reviewed and the initial results of our investigation of the Np–Fe system are presented. The results of a simple regular-solution alloy model are considered in relation to the magnitude of 5f bonding in the light actinides to explain some of our observations on the alloying behavior of neptunium.

3.1. The Np–Zr and Np–Am alloy systems

We previously reported on DTA investigations of phase relationships in the Np–Am [3] and Np–Zr [4, 5] systems. Although these data were insufficient for constructing detailed phase diagrams, they did establish the essential constitutions of the diagrams.

For the Np–Am system, the transition temperatures of each component were only slightly affected by saturation with the other, and the phase diagram was characterized as immiscible. Although this finding was in striking contrast to the extensive miscibility found in the Pu–Am system [7], it was in accord with predictions based upon a regular-solution model [8]. The lack of experimental information for the U–Am system precluded any comparison there. A refined Np–Am phase diagram recently presented by Ogawa [9] is consistent with our DTA results for this system.

In the case of the Np–Zr system, the DTA results [4, 5] also suggested immiscibility. For example, the melting point of Np was found to be essentially invariant (to within a few degrees Celsius) on addition of more than 20 at.% Zr. This result was unanticipated by analogy with U–Zr [10] and Pu–Zr [11]; rather it had been expected that the high temperature b.c.c. forms of Np and Zr would be miscible, and that the melting of Np would be dramatically elevated by the addition of Zr (by at least 100 °C on addition of 10 at.% Zr). Regular-solution modeling of the Np–Zr system [8] also predicted b.c.c. miscibility there, and substantial melting point elevation of the resulting solid solution relative to pure Np.

As we proposed previously [5], the Np–Zr phase diagram may resemble the largely immiscible U–Th diagram [12]. In Fig. 1 is presented a general form for the Np–Zr phase diagram which is consistent with our experimental findings. This diagram incorporates features (*e.g.* the intermetallic phase, Np_4Zr) suggested by recent XRD results which will be reported elsewhere [13]. It must be emphasized that several of the details

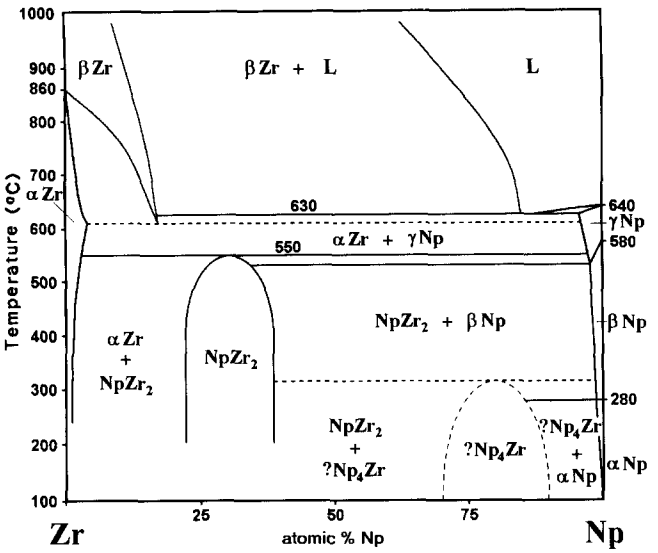

Fig. 1. Postulated general form of the Np–Zr phase diagram.

of this diagram are speculative; the key feature indicated by the DTA results was the immiscibility of the high temperature b.c.c. phases of Np (γ-Np) and Zr (β-Zr).

3.2. The Np–Fe alloy system

We recently studied the phase relations in the Np–Fe system. The U–Fe and Pu–Fe phase diagrams [14] are similar to one another and indicate immiscibility of the terminal (elemental) phases and formation of An–Fe intermetallic phases. Each diagram is characterized by two compounds: the $AnFe_2$, both of which melt congruently near 1240 °C; and the An_6Fe, both of which decompose peritectically (at 810 °C for U_6Fe and 428 °C for Pu_6Fe). Each diagram also exhibits an iron-rich eutectic around 1100 °C, and an actinide-rich eutectic (at 725 °C for U and 410 °C for Pu). Given the position of Np between U and Pu in the actinide series, it was expected that the Np–Fe diagram would be comparable with the U–Fe and Pu–Fe diagrams, and that the Np–Fe transition temperatures would be intermediate between those for U–Fe and Pu–Fe.

Of particular interest in establishing the behavior of the Np–Fe system relative to the U–Fe and Pu–Fe systems was the determination of the incongruent melting temperature of Np_6Fe, which intermetallic phase had been reported previously on the basis of XRD studies [15]. Np–Fe alloy samples with aggregate compositions of 24 and 29 at.% Fe were investigated in our initial DTA studies. Both aggregates exhibited a transition near 540 °C, which was not observed with pure Np. By analogy with the U–Fe and Pu–Fe phase diagrams, we have tentatively assigned this transition as the approximate peritectic decomposition temperature for the compound, Np_6Fe. This transition tem-

perature is intermediate between those reported for U_6Fe (810 °C) and Pu_6Fe (410 °C); however, it is substantially closer to the Pu_6Fe peritectic temperature than to that for U_6Fe. Additional studies of the Np–Fe system will be aimed at further elucidating the phase diagram and establishing the extent of the similarities between the three binary alloy systems, U–Fe, Np–Fe and Pu–Fe.

3.3. The role of 5f bonding in actinide alloying behavior

We suggested previously [5] that the role of 5f electrons in metallic bonding in the light actinides might be invoked to explain the observed unique and unexpected behavior in the Np–Zr system. Such 5f bonding effects would be relevant to predicting and understanding phase diagrams that include a light actinide, which exhibits significant 5f bonding in its elemental state.

The involvement of 5f electrons in bonding in the actinides, U, Np and Pu, is well recognized [2]. The bonding due to 5f electrons becomes ineffective when the An–An distances exceed a critical value, and 5f bonding is therefore non-existent in most compounds of the lighter actinides. A similar disruption in 5f bonding is expected when a 5f-bonded actinide metal is spatially dispersed by alloying with a non-5f-bonded metal. Brewer [16] has assigned values for the contribution of the 5f electrons to the net metallic bonding in the actinide elements. A consideration of these values, in comparison with estimated free energies of alloying, allows an assessment of 5f bonding effects in determining the resistance of U, Np and Pu to alloying with a non-5f-bonded element.

To assess the importance of 5f bonding in light actinide alloying behavior, we have invoked the regular-solution model and the van Laar expression for the binary interaction parameter to estimate the approximate excess free energy $\Delta_m^E G$ of alloying [17]. For an equimolar binary alloy, $M^1_{0.5}M^2_{0.5}$, the free energy is given by the relation

$$\delta_m^E G = Q_{12} V_1 V_2/(V_1+V_2) \quad (1)$$

In this expression, V_i is the molar volume of pure component i and Q_{12} is the symmetrical binary interaction parameter, given by

$$Q_{12} = (1/2)[(\Delta E_1/V_1)^{1/2} - (\Delta E_2/V_2)^{1/2}]^2 \quad (2)$$

The ΔE_i in eqn. (2) are typically taken as the molar energies of vaporization (to the atomic ground state electronic configuration) of component i [17]. However, Brewer [16] has shown that a more appropriate quantity to use there is the hypothetical energy of vaporization from the condensed metallic state to the atomic state with the same electronic configuration (designated $\Delta^* E_i$); this approach invokes the atomic promotion energy to the metallic valence configuration as an adjustment to the measured vaporization energy.

In Table 1 are given the thermodynamic properties of the elements used to calculate the excess free energy of alloying; also given are the corresponding 5f bonding contributions $\Delta_{5f}E$ to the elemental cohesive energies, as suggested by Brewer [16]. For simplicity, room temperature molar volumes $V°$ have been used and the unadjusted cohesive energies ΔE were taken as the $\Delta_v H°_{298}$. The cohesive energies, adjusted for the change in electronic configuration on vaporization ($\Delta^* E$), were taken as equal to the sum of ΔE and the atomic promotion energy to the configuration for the b.c.c. (d.h.c.p. for Am) metallic valence state. Although a more rigorous application of the regular-solution model would consider the temperature dependence of the parameters, this simplified treatment is sufficient to estimate the approximate relative tendencies for alloy-pair demixing. The resulting regular solution interaction parameters Q and Q^* and the corresponding excess free energies $\Delta_m^E G$ and $\Delta_m^{*E} G$ of mixing for selected equimolar binary alloys ($M^1_{0.5}M^2_{0.5}$) are given in Table 2. The equimolar alloy composition was arbitrarily selected to provide a representative indication of the tendency for solid solution formation. The net free energy $\Delta_m G$ of mixing will consist of the sum of the excess free energy and the ideal free energy of mixing:

$$\Delta_m G = \Delta_m^E G + \Delta_m^{Id} G = \Delta_m^E G - T\,\Delta_m^{Id} S \quad (3)$$

TABLE 1. Elemental properties

	$V°_{298}$ (cm^3 mol^{-1}) [18, 19]	$\Delta_v H°_{298}$ (kJ mol^{-1}) [20, 21]	$\Delta^* E$ [a] (kJ mol^{-1})	$\Delta_{5f}E$ (kJ mol^{-1}) [16]
U	12.50	536	720	50
Np	11.56	465	750	70
Pu	12.04	342	556	40
Am	17.64	284	644	?
Zr	14.03	612	706	–
Fe	7.095	398	555	–

[a]Brewer's $\Delta^* E$ [16] have been adjusted for consistency with these $\Delta_v H°$.

TABLE 2. Interaction parameters and excess free energies for $M^1_{0.5}M^2_{0.5}$

M^1–M^2	Q (J cm^{-3})	$\Delta_m{}^E G$ (J mol^{-1})	Q^* (J cm^{-3})	$\Delta^*{}_m{}^E G$ (J mol^{-1})
U–Zr	2	13	123	813
Np–Zr	34	215	462	2930
Pu–Zr	813	5270	44	285
Am–Zr	3360	26260	553	4320
Np–Am	2710	18930	2030	14180
Pu–Am	868	6210	284	2030
Np–Fe	658	2890	312	1370

For an equimolar binary alloy, the ideal free energy term is given by $-T\,\Delta_m^{Id}S = -RT\ln(0.5)$; the value of this term is -1720 J mol^{-1} at 298 K, and -5760 J mol^{-1} at 1000 K.

The large discrepancies between the $\Delta_m^{*E}G$ and $\Delta_m^{E}G$ values for several of the alloy pairs in Table 2 illustrates the potential for the significant effects in alloy modeling of the substantial differences between the actual solid state cohesive energies Δ^*E and those inferred from the uncorrected vaporization energies ($\Delta E \approx \Delta_v H$). For example, for the Am–Zr system the large value for $\Delta_m^{E}G$ (26 260 J mol^{-1}) would unambiguously predict immiscibility, whereas the much smaller value for $\Delta_m^{*E}G$ (4320 J mol^{-1}) is less conclusive and suggests the possibility of solid solution formation. In accord with the rationale elucidated by Brewer [22], the $\Delta_m^{*E}G$ values better represent the actual cohesive energy in the condensed state and are to be considered more relevant to predicting alloying behavior.

Given the magnitude of $\Delta_m^{Id}G$ (*e.g.* -10 kJ mol^{-1} for $T = 1700$ K), it is evident for the alloy pairs considered here that only in the case of the Np–Am system does the calculation (Table 2; $\Delta_m^{*E}G$(Np–Am) = 14 180 J mol^{-1}) clearly indicate immiscibility. This prediction of the simple regular-solution model is consistent with our experimental findings for the Np–Am system. In contrast to the Np–Am system, but in accord with the previous experimental results [7], the calculated value of $\Delta_m^{*E}G$ for Pu–Am (2030 J mol^{-1}) predicts miscibility.

Although the calculated $\Delta_m^{*E}G$ for Np–Fe is only moderately positive (1370 J mol^{-1}), this alloy pair is characterized by a substantial radius mismatch (see the volumes given in Table 1) and dissimilar electronegativities. Furthermore, the known formation of intermetallic Np–Fe phases suggests a more complex bonding interaction in this alloy system than is considered by the rudimentary regular-solution model. The inability to predict the essential nature of the Np–Fe diagram exemplifies that the results of the simple regular-solution model are of limited relevance when the properties of the components (*e.g.* radii, electronegativities, electron affinities) are substantially dissimilar.

The small $\Delta_m^{*E}G$ values calculated (Table 2) for U–Zr (183 J mol^{-1}) and Pu–Zr (285 J mol^{-1}) predict solid solution formation, consistent with the known phase relations [10, 11]. The corresponding value for Np–Zr (2930 J mol^{-1}), although significantly larger, is actually only slightly less favorable for mixing, and would suggest at least high temperature miscibility. However, the approximate values for $\Delta_{5f}E$ suggested by Brewer [16] for U, Np and Pu (Table 1) would predict an additional, significant demixing tendency on non-5f bonding alloying (*e.g.* with Zr), which is not incorporated into the simple regular-solution model. Furthermore, this 5f-bond-breaking influence should be most significant for Np, and may be of a magnitude substantially greater (*e.g.*, 10 kJ mol^{-1}) than other alloying effects. Considering this additional (anti-) bonding factor, not included in previous predictions of phase relations in the Np–Zr system, it may be entirely reasonable retrospectively that the Np–Zr system, unlike the U–Zr and Pu–Zr systems, is actually characterized by immiscibility.

4. Conclusion

This discussion of regular-solution model predictions of essential alloying behavior, and the influences of additional, "higher-order", metallic bonding effects, serves to re-emphasize the necessity for empirical determinations of phase relations in actinide alloy systems as a basis for understanding and predicting alloying behavior.

Acknowledgments

This work was sponsored by the Division of Chemical Sciences, Office of Basic Energy Sciences, US Department of Energy, under Contract DE-AC0584-OR21400 with Martin Marietta Energy Systems, Inc. (MMES) and by the Japan Atomic Energy Research Institute (JAERI) under the Japan–US Actinide Program. The authors are grateful for the ongoing contributions and support of actinide alloy studies by Drs. T. Mukaiyama of JAERI and S. Raman of MMES.

References

1 P. Chiotti, V.V. Akhachinskij, I. Ansara and M.H. Rand, *The Chemical Thermodynamics of Actinide Elements and Compounds,* Part 5, *The Actinide Binary Alloys,* International Atomic Energy Agency, Vienna, 1981.
2 J.L. Smith and E.A. Kmetko, *J. Less-Common Met., 90* (1983) 83.
3 J.K. Gibson and R.G. Haire, *J. Nucl. Mater., 195* (1992) 156.
4 J.K. Gibson and R.G. Haire, *Thermochim. Acta., 207* (1992) 65.
5 J.K. Gibson and R.G. Haire, *J. Nucl. Mater., 201* (1993) 225.
6 J.K. Gibson, R.G. Haire, M.M. Gensini, E.C. Beahm, A. Maeda and T. Ogawa, submitted for publication.
7 F.H. Ellinger, K.A. Johnson and V.O. Struebing, *J. Nucl. Mater., 20* (1966) 83.
8 E.C. Beahm, Oak Ridge National Laboratory, personal communication, 1989.
9 T. Ogawa, *J. Alloys Comp., 194* (1993) 1.
10 H. Okamoto, *J. Phase Equilib., 13* (1992) 109.
11 C.B. Alcock, K.T. Jacob, S. Zador, O. Kubaschewski von Goldbeck, H. Nowotny, K. Seifert and O. Kubaschewski, in O. Kubaschewski (ed.), *Zirconium: Physico-chemical Properties of its Compounds and Alloys,* Special Issue No. 6, International Atomic Energy Agency, Vienna, 1976, pp. 108–111.

12 D.E. Peterson, *Bull. Alloy Phase Diagr., 6* (1985) 443.
13 M.M. Gensini, R.G. Haire and J.K. Gibson, *J. Alloys Comp.,*.
14 O. Kubaschewski, *Iron – Binary Phase Diagrams,* Springer, New York, 1982, pp. 94–96, 157–160.
15 B.C. Giessen, R.B. Roof, A.M. Russell and R.O. Elliott, *J. Less-Common Met., 53* (1977) 147.
16 L. Brewer, *The Cohesive Energies of the Elements, Rep. LBL-3720 Rev.,* 1977 (Lawrence Berkeley Laboratory, CA).
17 G.N. Lewis, M. Randall, K.S. Pitzer and L. Brewer, *Thermodynamics,* McGraw-Hill, New York, 2nd edn., 1961, pp. 282–290.
18 W.H. Zachariasen, *J. Inorg. Nucl. Chem., 35* (1973) 3487.
19 C. Kittel, *Introduction to Solid State Physics,* Wiley, New York, 5th edn., 1976.
20 J.J. Katz, G.T. Seaborg and L.R. Morss, *The Chemistry of the Actinide Elements,* Vol. 2, Chapman and Hall, New York, 1986, pp. 1121–1195.
21 O. Kubaschewski and C.B. Alcock, *Metallurgical Thermochemistry,* Pergamon, New York, 5th edn., 1979, pp. 358–377.
22 L. Brewer, in P. Rudman, J. Stringer and R.I. Jaffee (eds.), *Phase Stability in Metals and Alloys,* McGraw-Hill, New York, 1967, pp. 39–61.